Supplement of Atmos. Chem. Phys. Discuss., 15, 2957–2996, 2015
http://www.atmos-chem-phys-discuss.net/15/2957/2015/
doi:10.5194/acpd-15-2957-2015-supplement

Atmospheric Chemistry and Physics Discussions

Supplement of

Photochemical processing of aqueous atmospheric brown carbon

R. Zhao et al.

Correspondence to: J. P. D. Abbatt (jabbatt@chem.utoronto.ca)

S1. Determination of Photon Flux in the Solar Simulator

The output of the solar simulator was recorded using the detector of the liquid waveguide capillary UV-Vis spectrometer described in the main article Section 2.2. This method qualitatively determines the spectral shape of the simulated sunlight.

Meanwhile, chemical actinometry using 2-nitrobenzaldehyde (2NB) was employed to quantitatively evaluate the simulated sunlight. This chemical actinometer has been employed previously by Anastasio and coworkers for quantification of photon flux in aqueous phase and ice. The absorption cross section, as well as the recommended quantum yield of this compound, are provided by Galbavy et al. (2012).

A 2NB solution (200 uM, 100 mL) was prepared and was illuminated in the solar simulator. Aliquots were taken every two minutes for offline analyses. Measurement of 2NB was conducted using a high performance liquid chromatography (HPLC) system equipped with a Perkin Elmer Series 200 pump, a Shimadzu SPD-10A UV-Vis detector, a Waters Symmetry® C18 column (5 µm pore size, 4.6 mm diameter and 150 mm column length). A mixture of acetonitrile and water (60 : 40) was used as the mobile phase in isocratic mode, with a flow rate of 1 mL / min. Absorption at 256 nm was monitored for the detection of 2NB.

Using the absorption cross section and recommended quantum yield of 2NB (Galbavy et al. 2010), we scaled the recorded output spectra from the solar simulator to match the observed decay rate of 2NB. The photon flux determined this way is shown in Fig. S1, along with ambient actinic flux at the Earth's surface with a zenith angle of 0 ˚ (Finlayson-Pitts and Pitts 2000).

The integrated photon flux between 290 and 380 nm is similar between the simulated and ambient photon flux. Although the simulator supplies more photo photons than the ambient at longer wavelengths, we assume that they are fairly similar, as we do not know what wavelengths are responsible for BrC photolysis (i.e. the quantum yields are unknown).

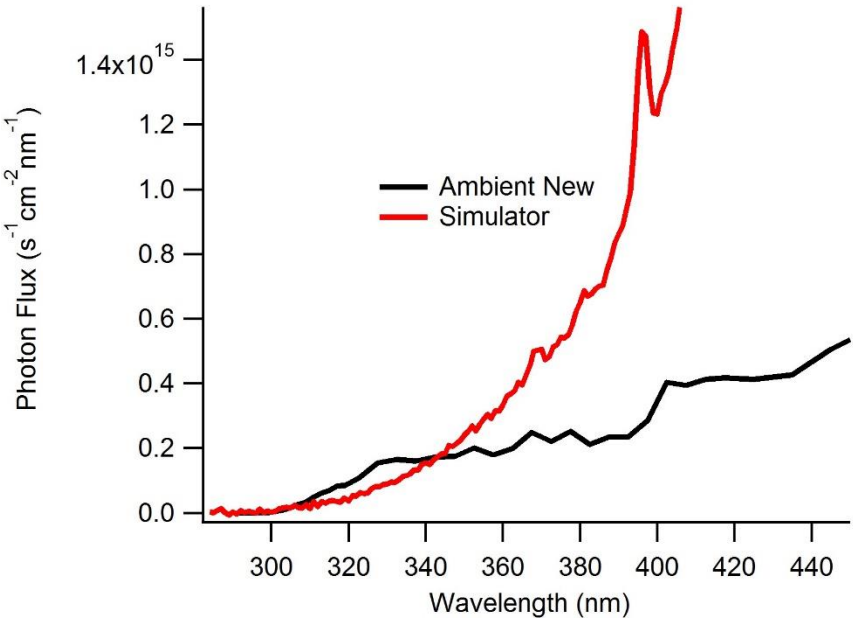

Fig. S1: The photon flux in the solar simulator and in the ambient.

S2. Quantitative Assessment of BrC Absorption

S2.1 Imine BrC

The mass absorption coefficients (MAC) of the GLYAS and MGAS solutions were calculated. While it is difficult to estimate the amount of BrC in the solution, we used the total organic carbon (TOC) content of the solution to calculate MAC. The concentrated stock solutions of GLYAS and MGAS were diluted by a factor of 100, and the TOC content of the diluted solutions was measured using a Shimadzu TOC-ICPH Total Organic Analyzer. The wavelength dependent $MAC_{(\lambda)}$ is calculated based on Eqn. S1 (Lee et al. 2014):

$$\mathrm{MAC}_{(\lambda)} = \frac{A_{(\lambda)} \times \ln(10)}{b \times C_{mass}}, \qquad \text{Eqn. S1}$$

where $A_{(\lambda)}$ is the base-10 absorbance observed at wavelength λ, b is the effective path length of the liquid capillary waveguide (50 cm), and C_{mass} is the mass concentration (g cm^{-3}) of total organic carbon in the solution. The $MAC_{(\lambda)}$ values of GLYAS and MGAS calculated using Eqn. S1 are shown in Fig. S2(a).

S2.2. WSOC from Biofuel Combustion Samples

Calculations of the MAC for the biofuel combustion samples are conducted based on the organic matter (OM) contents measured by an OM/OC method described by Chan et al. (2010). $MAC_{(\lambda)}$ was calculated similar to Imine BrC using Eqn. S1 and is shown in Fig. S2(b). We consider the MAC determined in the current method a lower limit for these sample because: 1) particles freshly emitted from BB likely contain a large fraction of non-light absorbing organic compounds (Chen and Bond 2010), and 2) WSOC presents only a fraction of the total OM content of the particle, and the extraction efficiency is unknown.

The Angstrom absorption coefficients (AAE) between 290 nm and 480 nm were calculated using Eqn. S2 (Chen and Bond 2010) and are reported in the main article:

$$AAE = \frac{\ln(MAC(\lambda 1)/MAC(\lambda 2))}{\ln(\lambda 1/\lambda 2)}. \qquad \text{Eqn. S2}$$

S2.3. Nitrophenols

Since the nitrophenols are pure compounds, their wavelength dependent molar absorptivity ($\varepsilon_{(\lambda)}$) and absorption cross section ($\sigma_{(\lambda)}$) are calculated based on Eqn. S3 and S4, respectively.

$$\varepsilon_{(\lambda)} = \frac{A_{(\lambda)}}{c \times b} \qquad \text{Eqn. S3}$$

$$\sigma_{(\lambda)} = 1.66 \times 10^{-21} \varepsilon \qquad \text{Eqn. S4}$$

Eqn. S3 is based on the Beer-Lambert law, where $A_{(\lambda)}$ is the base-10 absorbance observed at wavelength λ, c is the molarity of the nitrophenol (M), and b is the effective path length of the liquid capillary waveguide (50 cm). Eqn. S4 converts $\varepsilon_{(\lambda)}$ to $\sigma_{(\lambda)}$ (both in base 10) (Finlayson-Pitts and Pitts, 2000). The calculated $\varepsilon_{(\lambda)}$ and $\sigma_{(\lambda)}$ are displayed in Fig. S2(c).

a) b)

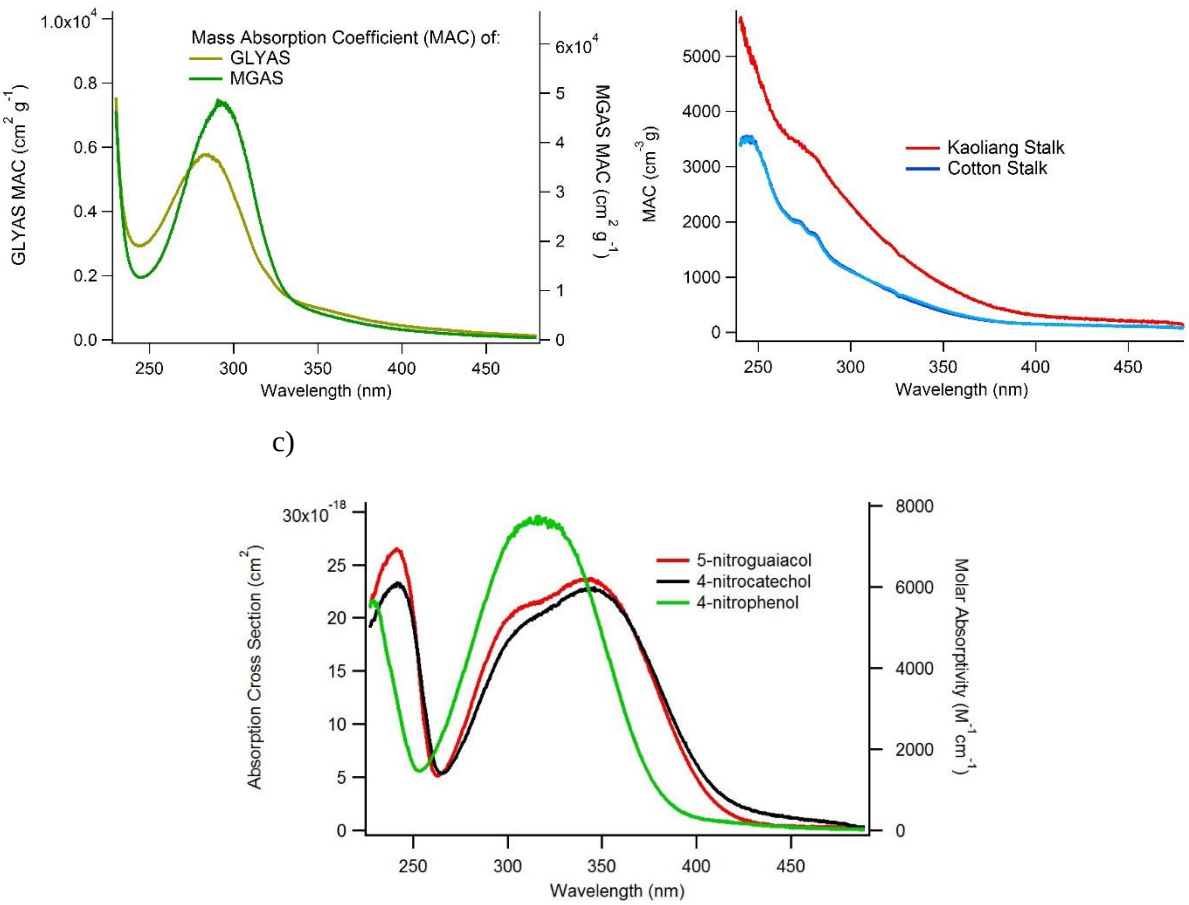

Fig. S2: Wavelength dependent mass absorption coefficient (MAC) for the Imine BrC (a), the WSOC from biofuel combustion samples (b), and the base 10 absorption cross section and molar absorptivity of the nitrophenols (c).

S3. Concentration Dependence of Imine BrC Decay Rate

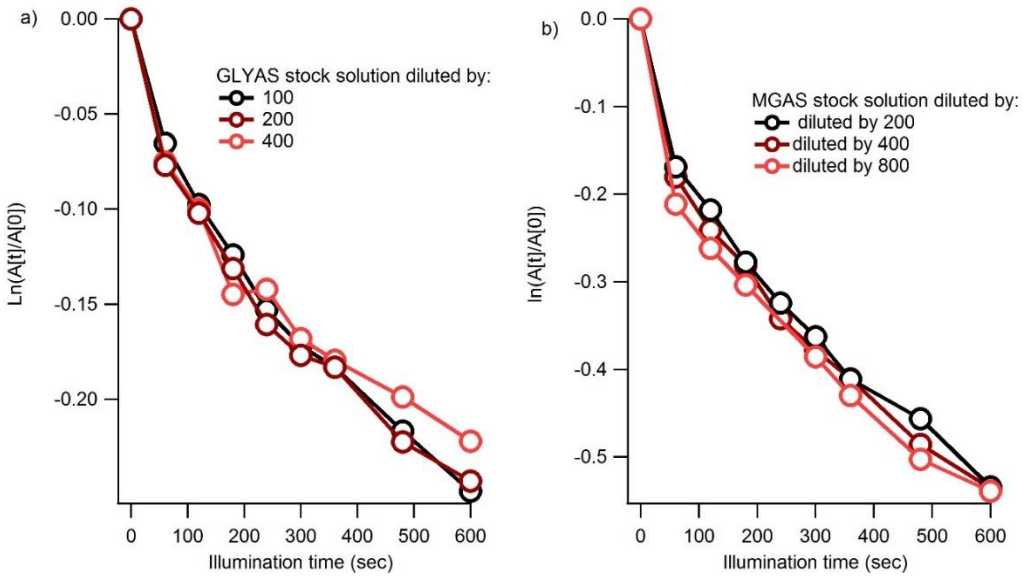

Fig. S3: Decay of the GLYAS solution (a) and the MGAS solution (b) during the first 10 min of illumination at different initial concentrations.

S4. Spectral Change of 4NP and 5NG during Direct Photolysis

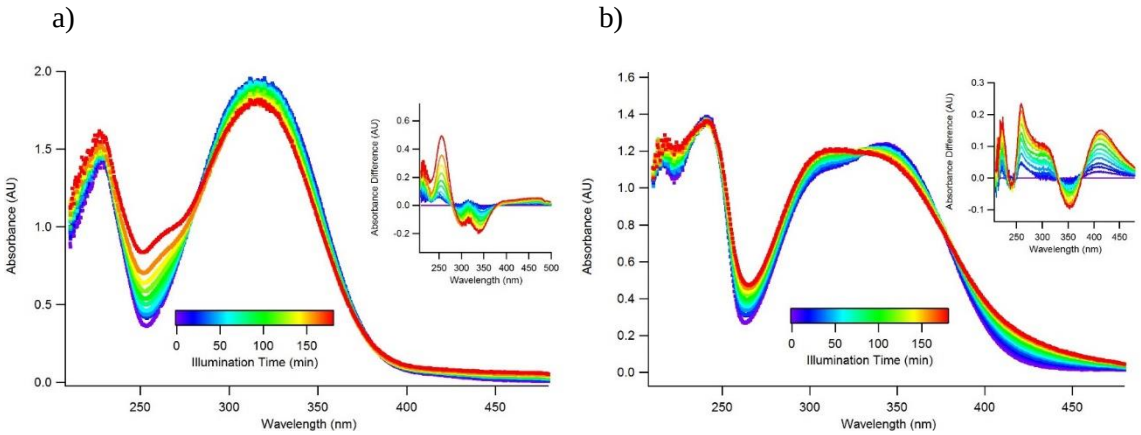

Fig. S4: Spectral change observed for a 4NP solution (a) and a 5NG solution (b) during direct photolysis experiments. The initial concentrations of 4NP and 5NG were 5 µM and 4 µM, respectively. The insets illustrate the absorbance change compared to the initial conditions.

S5. pH Dependent Photo-enhancement of 4NP and 5NG and OH Scavenger Experiments

We investigated the photo-enhancement of the nitrophenols at solution pH of 3, 4 and 5. We also conducted an OH scavenger experiment where glyoxal (1 mM) was added to a pH 5 solution to react OH radicals away.

The OH scavenger experiment affects the photo-enhancement rate of 4NP, but did not completely shut down the reaction. 5NG was not affected by the OH scavenger. The photo-enhancement rate of 4NP at 420 nm exhibited irregularity (Fig. S5(a)), perhaps due to the fact that 420 nm was close to the isosbestic point of 4NP absorption. When we plotted the photo-enhancement of 4NP at a longer wavelength, 450 nm (Fig. S5(b)), we observed a clearer pH dependence. 5NG exhibited a unique pH dependence (Fig. S5(c)), where the photo-enhancement was suppressed significantly when the pH was 3.

For 4NP and 5NG, the formation of color exhibited strong linearity in time, which prevented us from fitting a 1st order growth curve to extract k^{I}_{direct}. Therefore, we decided to present the rate of photo-enhancement (k^{*}_{direct}) in an absorbance based manner using Eqn. S5 in units of [AU M^{-1} s^{-1}]:

$$k^{*}_{direct} = S/60 \times C_{ini} \qquad \text{Eqn. S5}$$

where S (AU min^{-1}) is the initial slope of color formation found from Fig. S5, 60 is the conversion factor from minutes to seconds, and C_{ini} (M) is the initial concentration of the nitrophenol. The k^{*}_{direct} values obtained are summarized in Table S1. If the identity and molar absorptivity of the reaction products are determined from future studies, these absorbance based rate constants can be converted into concentration based constants.

Table S1: The absorbance based 1st order rate constant of photo-enhancement

		k^{*}_{direct} (AU M^{-1} s^{-1})			
Compound	C_{ini} (µM)	pH3	pH4	pH 5	pH 5 OH scav.

4NP (420 nm)	15	0.68	0.62	0.40	0.24
4NP (450nm)	15	0.37	0.47	0.64	0.47
5NG (420 nm)	8	2.7	4.0	4.8	4.8

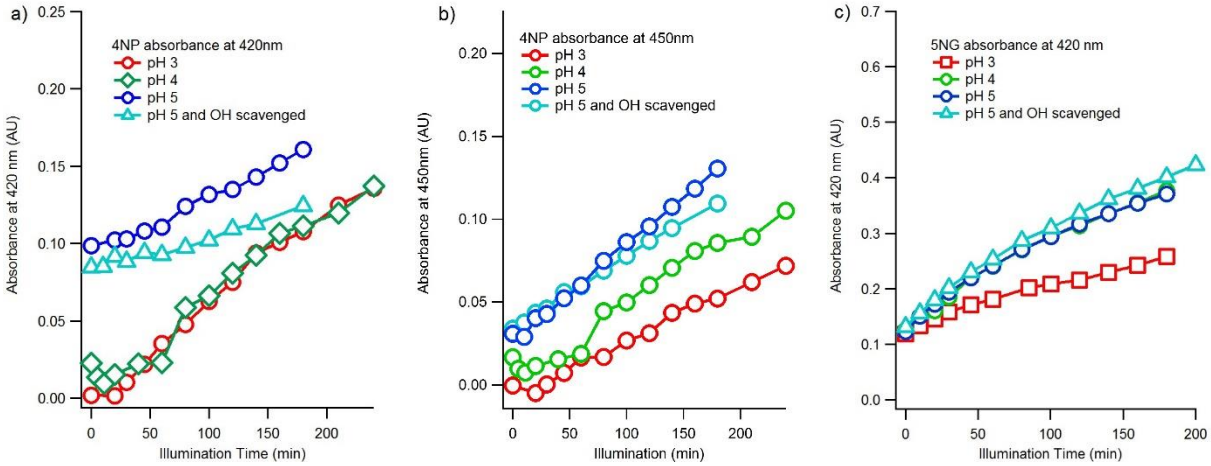

Fig. S5: Color formation from 4NP and 5NG solutions during the pH dependent and the OH scavenger experiments. The formation profiles of absorbance at 420 nm and 450 nm from 4NP are shown in (a) and (b). The formation profiles of absorbance at 420 nm from 5NG are shown in (c).

S6. pH Dependent Absorption of Nitrophenols

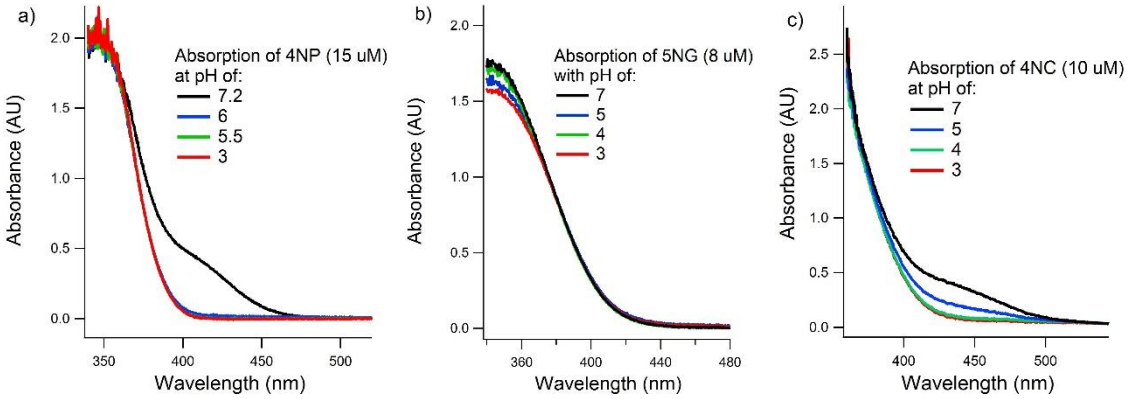

Fig. S6: Absorption spectra of 4NP (a), 5NG (b) and 4NC (c) at various solution pH values.

S7. Photooxidation of 4NP and 5NG

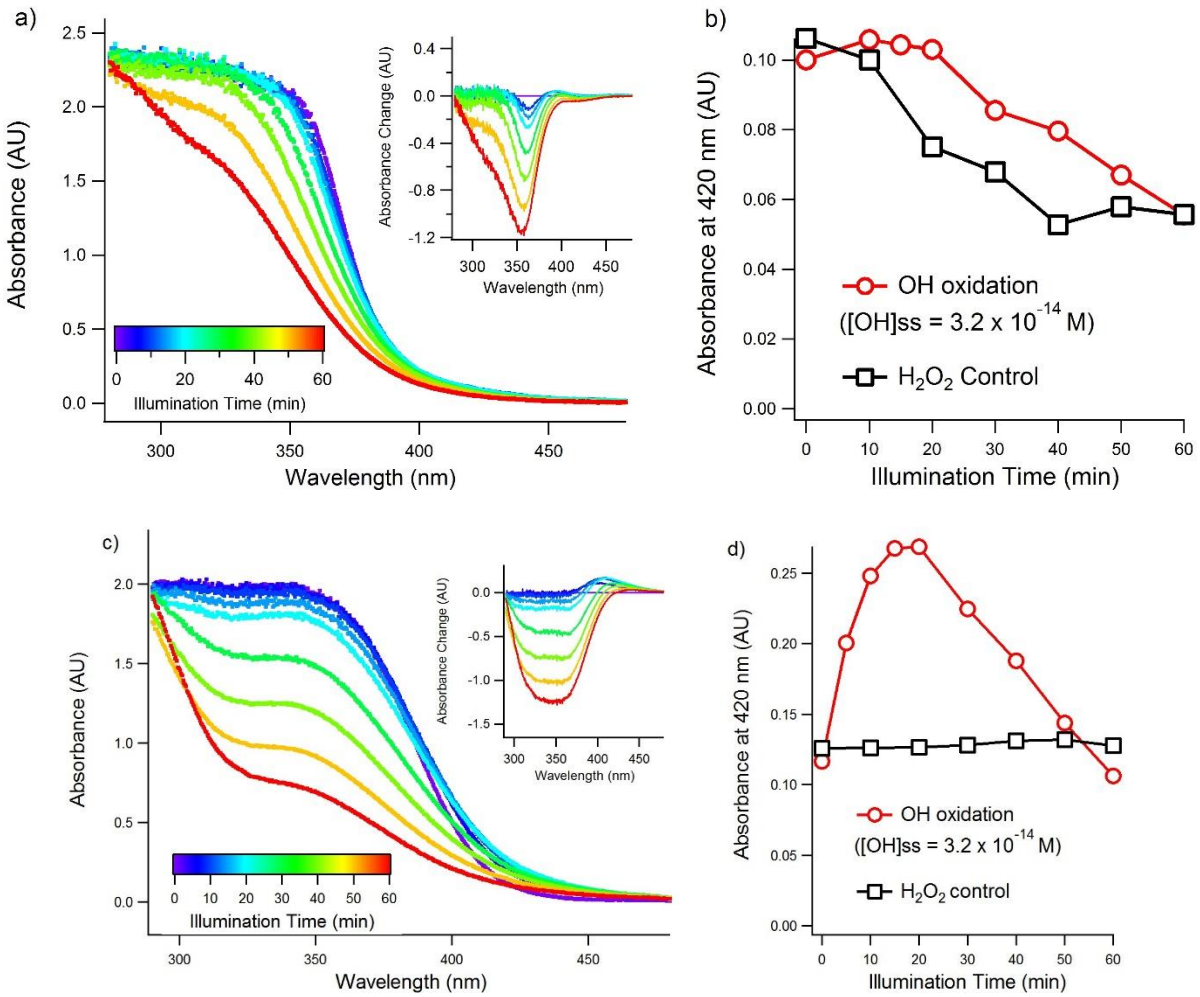

Fig. S7: The spectral change of 4NP and 5NG solutions during OH oxidation experiments are shown in (a) and (c). The time profiles of absorbance at 420 nm for 4NP and 5NG are shown in (b) and (d). In (b) and (d), the black traces represent H_2O_2 control experiments, while the red traces represent OH oxidation experiments. The concentration of 4NP and 5NG solutions are 15 µM and 8 µM, respectively.

S8. Simple Kinetic Model Applied to 4NP and 5NG

In this model, the precursor nitrophenols undergo prescribed pseudo-1st order decay with a [OH]ss of 3.2 × 10^{-14} M. For the case of 4NP we also observed direct loss by photolysis (Fig. S7(b)) by the 254 nm lamp with a rate constant of 2.6 × 10^{-4} s^{-1}. This direct photolysis was also added to the prescribed decay of 4NP. The 2nd order rate constant of 4NP was adopted from Einschlag et al. (2003): 6.2 × 10^{9} M^{-1} s^{-1}. Although the OH reactivity of 5NG and 4NC in the aqueous phase is not available in the literature, we used 1 × 10^{10} M^{-1} s^{-1} as a rough estimate for these two compounds. This estimation is based on the fact that the additional methoxy and hydroxy functional groups on 5NG and 4NC are electron donating and can likely enhance the OH reactivity. The model results for sample 4NP and 5NG OH oxidation experiments are shown in Fig. S8.

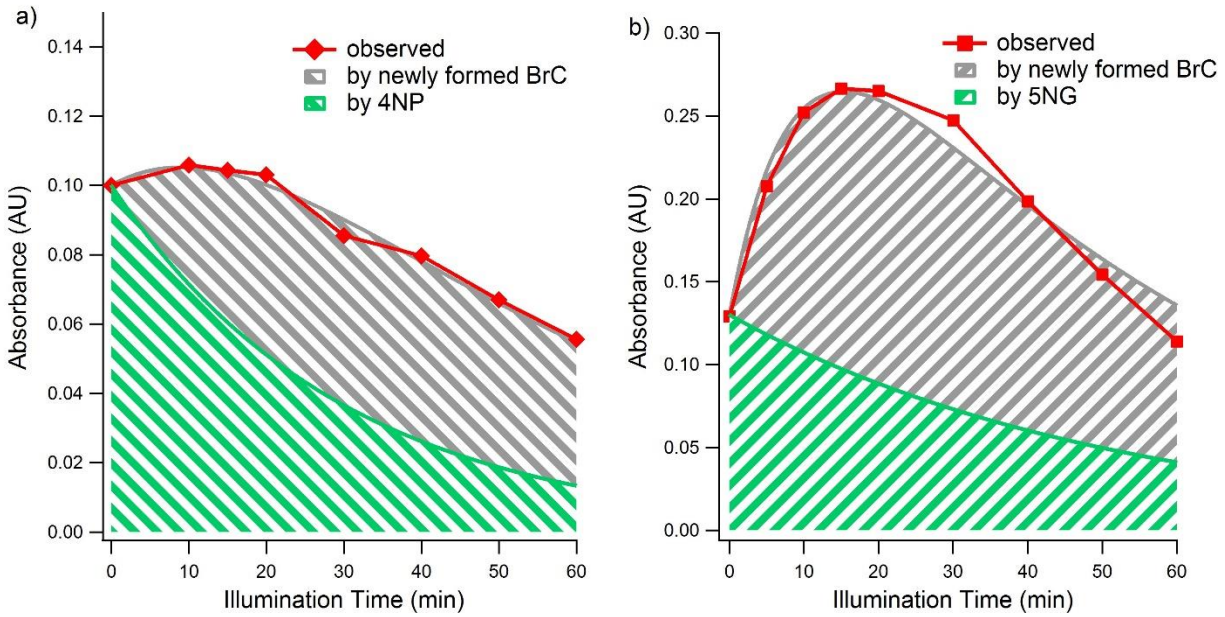

Fig. S8: The simple kinetic model applied to one example experiment each of 4NP (a) and 5NG (b) OH oxidation. The shaded areas are the simulated contribution of a newly formed colored product and the decay precursor. The red lines represent the experimental results.

References:

Chan, T. W., Huang, L., Leaitch, W. R., Sharma, S., Brook, J. R., Slowik, J. G., Abbatt, J. P. D., Brickell, P. C., Liggio, J. and Li, S.: Observations of OM/OC and specific attenuation coefficients (SAC) in ambient fine PM at a rural site in central Ontario, Canada, Atmos. Chem. Phys., 10, 2393-2411, 2010.

Chen, Y. and Bond, T.: Light absorption by organic carbon from wood combustion, Atmos. Chem. Phys., 10, 1773-1787, 2010.

Einschlag, F. S. G., Carlos, L. and Capparelli, A. L.: Competition kinetics using the UV/H2O2 process: a structure reactivity correlation for the rate constants of hydroxyl radicals toward nitroaromatic compounds., Chemosphere, 53, 1-7, 2003.

Finlayson-Pitts, B. J. and Pitts, J. N.: Chemistry of the upper and lower atmosphere : theory, experiments and applications, Academic Press, San Diego, Calif. ; London, 2000.

Galbavy, E. S., Ram, K. and Anastasio, C.: 2-Nitrobenzaldehyde as a chemical actinometer for solution and ice photochemistry, J. Photochem. Photobiol. A., 209, 186-192, 2010.

Lee, H. J., Aiona, P. K., Laskin, A., Laskin, J. and Nizkorodov, S. A.: Effect of solar radiation on the optical properties and molecular composition of laboratory proxies of atmospheric brown carbon, Environ. Sci. Technol., 48, 10217-10226, 2014.